IOP PUBLISHING JOURNAL OF PHYSICS D: APPLIED PHYSICS

J. Phys. D: Appl. Phys. **41** (2008) 074027 (5pp) doi:10.1088/0022-3727/41/7/074027

Investigations on indentation size effects using a pile-up corrected hardness

Y H Lee[1], J H Hahn[2], S H Nahm[1], J I Jang[3] and D Kwon[4]

[1] Division of Metrology for Quality Life, Korea Research Institute of Standards and Science, Daejeon 305-340, Korea
[2] Division of Advanced Technology, Korea Research Institute of Standards and Science, Daejeon 305-340, Korea
[3] Department of Materials Science and Engineering, Hanyang University, Seoul 133-791, Korea
[4] School of Materials Science and Engineering, Seoul National University, Seoul 151-742, Korea

Received 6 August 2007, in final form 1 October 2007
Published 12 March 2008
Online at stacks.iop.org/JPhysD/41/074027

Abstract
Indentation size effects (ISEs) become severe in the nanoindentation regime because various influencing factors become active in a very shallow indentation regime. Additionally, the general analysis on the nanoindentation curve yields hardness overestimation because it cannot take into account material pile-up around contacts. Thus we tried to investigate intrinsic ISEs in monolithic materials by proposing a new hardness measurement method; the load-supporting contact boundary was approximated as the peak trajectory around an impression and analysed by a radial differentiation of the remnant indent morphology. Dependence of the new load-off hardness on the indentation depth was investigated for (1 0 0) tungsten single crystal and fused quartz. The contribution of the material pile-up to the new hardness was clearly modified but more significant hardness increase appeared at a very shallow indentation regime due to severe elastic recovery. These phenomena are discussed with the strain-gradient plasticity model.

(Some figures in this article are in colour only in the electronic version)

1. Introduction

Nanoindentation measuring applied load and indentation depth during a contact deformation is one of the most powerful techniques for evaluating the mechanical properties of thin films and small volumes of materials [1–4]. Typical nanoindentation studies focus on the determination of hardness and Young's modulus. The hardness H is defined by equation (1).

$$H = \frac{L_{\max}}{A_C}, \tag{1}$$

where $L_{\max}$ and A_C are the peak indentation load and the contact area, respectively.

Young's modulus is also formulated with the terms of the nanoindentation unloading slope S and contact area A_C. Thus, the determination of A_C is crucial to the contact property analysis.

However, since the deformation morphology under indentation loads of less than mN cannot be easily observed, various models [1–4] for characterizing A_C at the peak indentation load from the nanoindentation curve have been developed. The method commonly used for analysing the nanoindentation load–depth curve is that proposed by Oliver and Pharr [2], expanding on an earlier work of Doerner and Nix [3]. Hereafter an analysis based on Oliver and Pharr's method is denoted as O&P. However it should be noted that the O&P method was developed from purely elastic contact mechanics [4] and that its applicability to complex elastic/plastic indentations of ductile metals has not been ascertained. If a plastic pile-up of material occurs around the indentation, the O&P method [2] can strongly underestimate the contact area, as reported in finite element simulation work [5]. Bolshakov and Pharr [5] note that only when $h_f/h_{\max}$ is smaller than 0.7 and the material shows significant elastic recovery after nanoindentation does the O&P method give a reasonable estimate of the contact area.

Some researchers [6–9] have proposed new indentation parameters, independent of the projected contact area, to characterize the mechanical properties. The elastic/plastic

loading curve of a homogeneous sample can be well described by a linear relationship between the indentation load L and the square of the indentation depth h^2 [6, 7]. And its slope, implying combined responses of the elasticity and plasticity of the sample, is formulated as the ratio of the reduced modulus to the contact hardness or E_r/H. Another parameter L_{max}/S^2 suggested by Joslin and Oliver [8] is linearly proportional to H/E_r^2 for a monolithic sample. If the hardness (or the reduced modulus) is already known or is estimated from a separate testing technique, the reduced modulus E_r (or the hardness H) can be evaluated from the elastic/plastic loading curve or the contact stiffness S of the unloading curve. However, measurement of the elastic modulus or contact hardness using another micromechanical technique is a somewhat difficult and cumbersome process. Lee *et al* [9] have proposed a new methodology for predicting the contact area by estimating Young's modulus of the sample independently from the Hertzian reversible loading part in the nanoindentation curve. However, the reversible loading part cannot be easily found from the nanoindentation curves obtained from sharp indentations on ductile metals.

The use of an atomic force microscope (AFM) or interferometer has thus been proposed to obtain the projected contact area of the ductile metal from direct observation of the residual impression [10–15]. Lim *et al* [10] analysed the indented surface of Al thin film on sapphire and determined the contact boundary as the fastest slope change inside the remnant indent. A similar study was performed by Sangwal *et al* [11] for MgO single crystals. However, this approach was proved to be effective for sink-in dominant materials [12]. Saha and Nix [13] tried to extract an approximate contact boundary by connecting few peak points identified from AFM line profiles. A few studies [14, 15] have also been done to form a smooth curve connecting two corners and centre peak of the indent baseline. The contact boundary, however, cannot be a smooth line and its morphology and trajectory depend on surface roughness, misaligned angle of the indenter axis and other influencing factors.

Thus, we proposed a new method to extract the pile-up corrected contact boundary by adopting a three-dimensional image analysis of the remnant indents. Peak points around a Berkovich indent consisting of the contact boundary were identified by radial differentiation. A distinctive contact boundary was determined between the inside and outside regions of the contact and finally the contact area was estimated by integrating the enveloped region. A new hardness was estimated and its indentation depth dependence was investigated by adopting a current model for indentation size effects (ISEs). Hereafter the analysis based on the proposed image differentiation is denoted as NEW.

2. Experiments

Two samples of fused quartz and tungsten single crystal representing sink-in dominant and pile-up dominant materials, respectively, were selected for the nanoindentation tests. Fused quartz in an amorphous state has been used as a standard sample for nanoindentation due to its isotropic deformation behaviour. The tungsten single crystal with negligible anisotropy has also been used for nanoindentation in order to avoid microstructural inhomogeneity of polycrystalline materials. While the fused quartz was prepared by a mirror-like mechanical polishing, the (1 0 0) crystallographic face of the tungsten single crystal (Goodfellow Cambridge Ltd, Huntingdon, UK) was mechanically ground and electrically polished in 2% NaOH aqueous solution at 6 V for 2 min.

The nanoindentation tests were carried out with a Nanoindenter II (MTS Instrument Corp., TN, USA) with a Berkovich diamond indenter. A detailed morphology of the indenter was embodied by a series of calibration tests on the standard fused quartz, and finally the contact area A_C was formulated in a series function of the contact depth h_C. Stepwise loads applied on the fused quartz were 1, 3, 6 and 10 mN and those on the tungsten single crystal were chosen as 0.8, 1.9, 3.8, 12.5, 42.2 and 175.7 mN in order to observe a clear variation of the hardness within a wide load range. Loading and unloading rates were commonly fixed as $2\,\mathrm{nm\,s^{-1}}$. More than five nanoindentation curves were recorded at each load step from various sample regions.

The indented surfaces were observed using a XE 100 atomic force microscope (PSIA Inc., Suwon, Korea) shortly after the nanoindentation tests. In order to obtain precise morphologies of the remnant indents, the AFM scanning speed is controlled at less than $5\,\mu\mathrm{m\,s^{-1}}$ and the pixel size of the AFM image is controlled at smaller than $15 \times 15\,\mathrm{nm^2}$. 3D morphology information on the indented surface was carefully levelled and then converted into a matrix-type ASCII file. The ASCII data was used as raw data for the subsequent Matlab image analyses.

3. Results and discussion

3.1. O&P hardness measured from the nanoindentation curve analysis

The nanoindentation curves obtained from both fused quartz and tungsten single crystal are superposed in figure 1. A low load regime of less than 10 mN is plotted in figure 1(*a*) while a high load regime of the tungsten sample is overlapped on figure 1(*b*). Good repeatability of the nanoindentation tests can be shown from the overlapping of the loading curves in figure 1. The unloading part after the peak indentation load in figure 1 is fitted to a power-law function of the indentation depth. The contact depth h_C is defined by $h_C = h_{max} - \omega L_{max}/S$, where h_{max} is the peak indentation depth and ω is the indenter geometry constant (for the three-sided Berkovich indenter, the value 0.72 for a conical indenter was used) [2]. h_C is converted into A_C using an empirical indenter shape; $A_C = C_0h_C^2 + C_1h_C + C_2h_C^{1/2} + C_3h_C^{1/4} + C_4h_C^{1/8} + C_5h_C^{1/16}$. In this study, the fitting constants C_0, C_1, C_2, C_3, C_4 and C_5 are taken as 25.76, 375.76, 7.94, 4.56×10^{-6}, 1.54×10^{-4} and 1.27×10^{-6}, respectively. The O&P hardness of the tungsten single crystal decreased from 6.88 ± 0.37 GPa at 0.9 mN to 4.04 ± 0.02 GPa at 175.7 mN due to the ISEs, while the hardness (O&P) of the fused quartz showed a slight decrease from 10.88 ± 0.10 GPa at 1 mN to 10.02 ± 0.22 GPa at 10 mN.

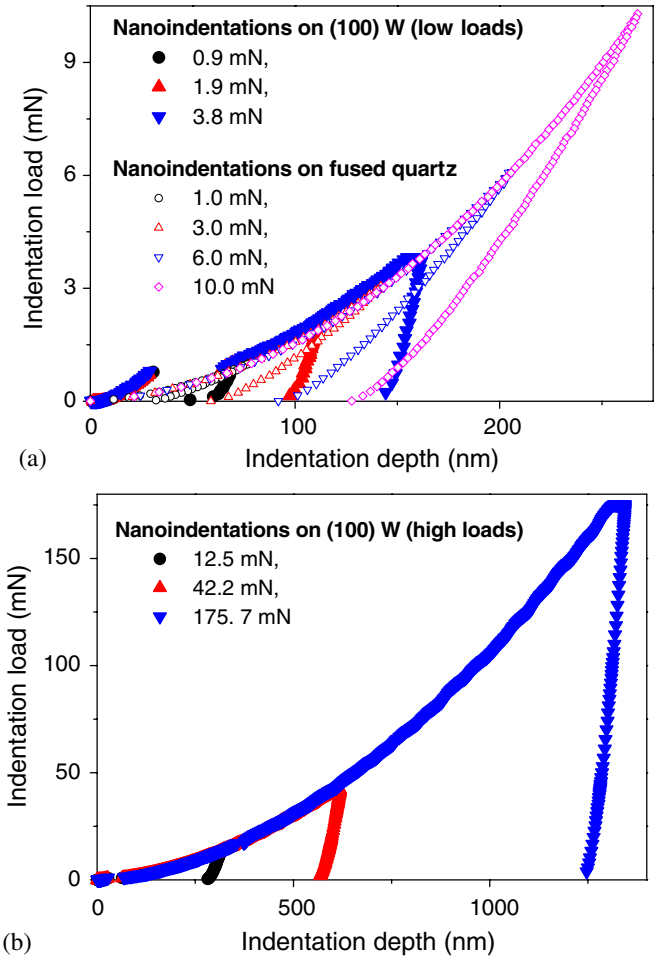

Figure 1. Nanoindentation load–depth curves obtained from fused quartz and tungsten single crystal; (*a*) low load regime less than 10 mN and (*b*) high load regime.

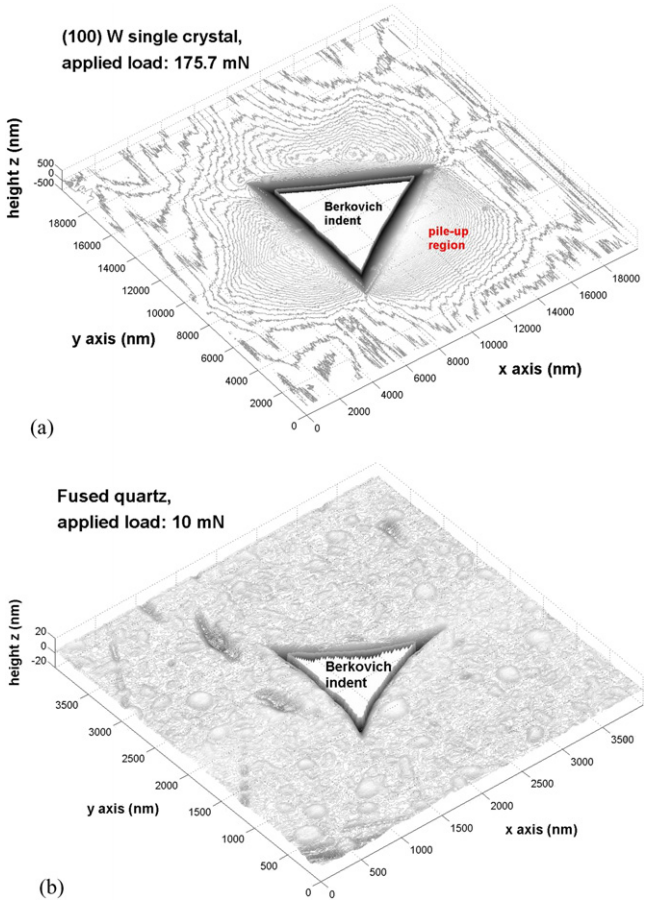

Figure 2. Three-dimensional morphologies of the remnant indents on (*a*) tungsten single crystal and (*b*) fused quartz.

3.2. NEW hardness measured from the remnant indent differentiation

Three-dimensional morphologies of the indented surface observed with the atomic force microscope are shown in figure 2. Significant material pile-up was observed around the indents on the tungsten single crystal while the indentation-induced surface upheaval was negligible in the fused quartz sample. In the present study, we assume that the contact boundary coincides with the peak point trajectory in the pile-up region similarly to previous studies [13–15] on indent observation. The three-dimensional deformation profiles obtained from the indented surface were differentiated with the radial distance from the indent centre. The differentiated images showed two discrete regions in figure 3: the white part flattened by the face of the sharp indenter and the complex tangled black/white parts formed by differentiating small asperities, which form the sample surface roughness.

The boundary between the two regions was traced and formed a closed loop of the contact boundary. The enveloped area within the closed loop was integrated and inserted into equation (1) in order to measure the NEW hardness. The differentiated image of nanoindent on the tungsten single crystal showed a convex-shaped contact boundary due to the contribution of the pile-up region, while the contact boundary of the fused quartz showed a concave shape due to significant sink-in and elastic recovery. The contact boundary determined in figure 3(*a*) is overlapped on a contour graph of the remnant indent in figure 4. As might be expected, the solid line passed through the peaks in the pile-up regions, confirming that our approach was reasonable. In addition, regardless of the difference in the deformation mode, the distinction between the white and black regions in figure 3(*b*) for the fused quartz is also clear. It means that this morphology differentiation method can be generally applied to any samples if a precise measurement on a remnant indent is provided.

The NEW hardness of the tungsten single crystal decreased from 8.16 ± 0.45 GPa at 0.9 mN to 3.30 ± 0.08 GPa at 175.7 mN due to the ISEs. For the fused quartz, the NEW hardness showed a slight decrease from 10.04 ± 0.13 GPa at 1 mN to 9.92 ± 0.05 GPa at 10 mN. Although both hardnesses from O&P and NEW analyses for the fused quartz showed nearly the same level, the NEW hardness of the tungsten single crystal was about 18.4% lower than the O&P hardness at an applied load of 175.7 mN. This hardness trend was reversed at low indentation load regime due to significant elastic recovery in the remnant indents. Thus the NEW hardness at 0.9 mN

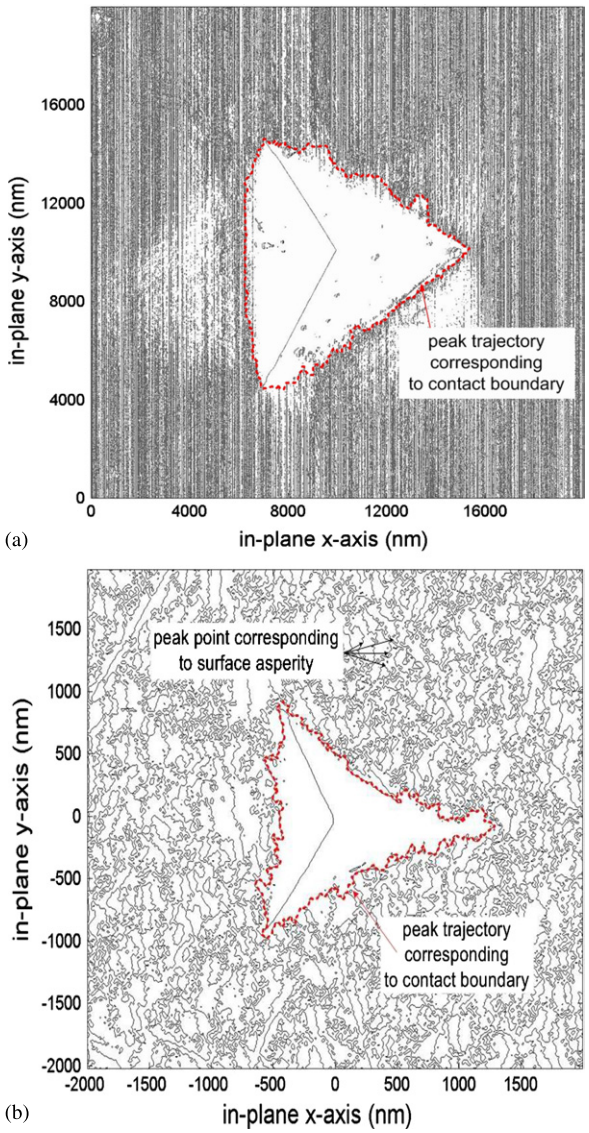

Figure 3. Differentiated images of the remnant indents on (*a*) tungsten single crystal and (*b*) fused quartz.

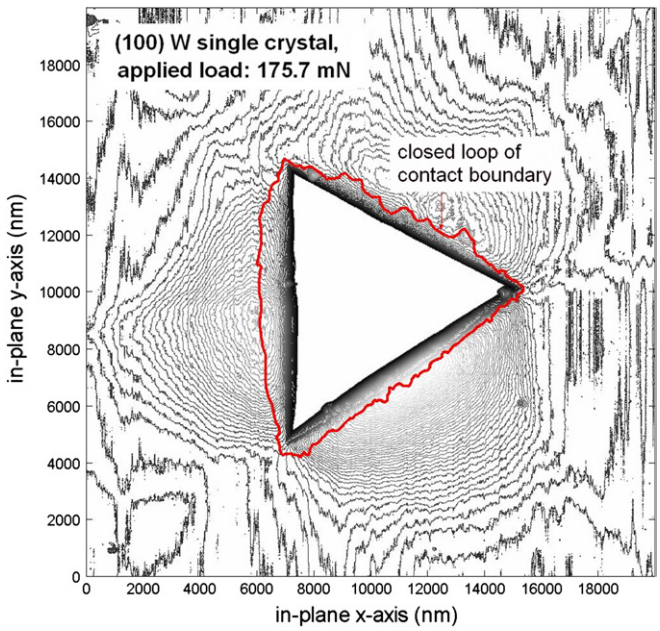

Figure 4. Superposition of the determined contact boundary on a two-dimensional contour graph of the nanoindent on the tungsten single crystal.

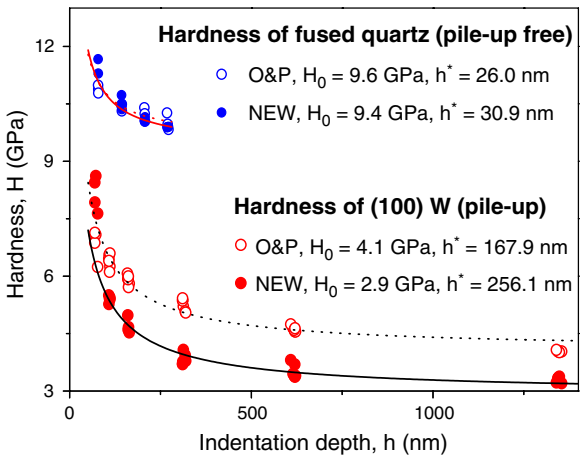

Figure 5. Hardness variations fitted into Nix and Gao's ISE model [16].

was about 18.6% higher than the O&P hardness in the tungsten single crystal (figure 5).

3.3. Analysis of the ISEs from the hardness variations

Nix and Gao [16] have proposed a model explaining the hardness decrease with indentation depth with a strain-gradient plasticity concept. The hardness is inversely proportional to the square root of the indentation depth, as shown in equation (2).

$$\frac{H}{H_0} = \sqrt{1 + \frac{h^*}{h}}, \tag{2}$$

where H_0 is the hardness value at infinite indentation depth and h^* is the characteristic length. All hardnesses measured from the two samples are plotted in figure 5 and fitted into equation (2). Although the hardness variation of the fused quartz cannot be explained with a dislocation accumulation mechanism, good fittings are achieved for O&P and NEW hardnesses. For fused quartz, inhomogeneous plastic deformation at the surface caused by indentation is not explained by geometrically necessary dislocation mechanism since it does not deform by the generation and propagation of dislocations. Nevertheless, small depth-dependent hardness of fused quartz describes the behaviour of intrinsically hard materials [16]. H_0 values from the two analyses coincided with each other within 2.1% and h^* values showed a 4.9 nm difference. It means the NEW hardness can converge to O&P hardness if the indentation depth is enough for a pile-up free material. For the tungsten single crystal, H_0 from the NEW hardness was about 1.2 GPa lower than the O&P result. This phenomenon is ascribed to the pile-up contribution and also affected the characteristic length. According to Nix and Gao's model [16], h^* has an inversely proportional relationship with H_0^2 and h^* of the NEW analysis showed about 52.5% higher

than that of the O&P analysis. This initiative study still needs wide application to various materials but flexibility of the indent image analysis to the hardness measurement was verified in both sink-in and pile-up dominant materials. In addition, basic research on the hardness and ISEs can be carried out by adopting the NEW analysis because the direct indent observation can exclude such factors as surface roughness [17], indenter imperfection [18] and curve analysis limitations.

4. Conclusions

In order to estimate the pile-up corrected hardness with the nanoindentation technique, a differentiation of the remnant indent morphology was proposed for an accurate determination of a closed contact boundary. This NEW method was applied to nanoindentation results from two samples of fused quartz and tungsten single crystal and compared with Oliver and Pharr's analyses for the same data. The important results are summarized below:

(1) A distinctive boundary was extracted from the differentiated indent image of the pile-up dominant tungsten single crystal. Furthermore, this contact boundary could also be derived from the fused quartz because a surface asperity flattening due to the nanoindentation clearly separated the inside and outside regions of the contact.
(2) The consistency of the NEW hardness with O&P hardness in the fused quartz confirms that our image analysis is valid for pile-up free materials. The O&P hardness measurement has been reported to be valid in these materials.
(3) By adopting the NEW analysis, the hardness at infinite depth of the tungsten single crystal was estimated at about 1.2 GPa lower than that of the O&P hardness variation. This is ascribed to the pile-up effects, and the NEW hardness at infinite depth was regarded as an intrinsic macrohardness of the tungsten single crystal.

Acknowledgments

This research was supported by a grant from the Center for Nanoscale Mechatronics & Manufacturing, one of the 21st Century Frontier Research Programs, which are supported by the Ministry of Science and Technology, Korea.

References

[1] Loubet J L, Georges J M and Meille J 1986 *ASTM STP 889: Nanoindentation Techniques in Materials Science and Engineering* (Philadelphia, PA: ASTM)
[2] Oliver W C and Pharr G M 1992 *J. Mater. Res.* **7** 1580
[3] Doerner M F and Nix W D 1986 *J. Mater. Res.* **1** 601
[4] Sneddon I N 1965 *Int. J. Eng. Sci.* **3** 47
[5] Bolshakov A and Pharr G M 1998 *J. Mater. Res.* **13** 1049
[6] Hainsworth S V, Chandler H W and Page T F 1996 *J. Mater. Res.* **11** 1987
[7] Malzbender J, de With G and den Toonder J M J 2000 *J. Mater. Res.* **15** 1209
[8] Joslin D L and Oliver W C 1990 *J. Mater. Res.* **5** 123
[9] Lee Y H, Baek U B, Kim Y I and Nahm S H 2007 *Mater. Lett.* **61** 4039
[10] Lim Y Y, Chaudhri M M and Enomoto T 1999 *J. Mater. Res.* **14** 2314
[11] Sangwal K, Gorostiza P, Servat J and Sanz F 1999 *J. Mater. Res.* **14** 3973
[12] Li Z, Cheng Y T, Yang H T and Chandrasekar S 2002 *Surf. Coat. Technol.* **154** 124
[13] Saha R and Nix W D 2001 *Mater. Sci. Eng.* A **319–321** 898
[14] Beegan D, Chowdhury S and Laugier M T 2003 *Surf. Coat. Technol.* **176** 124
[15] Kese K and Li Z C 2006 *Scr. Mater.* **55** 699
[16] Nix W D and Gao H 1998 *J. Mech. Phys. Solids* **46** 411
[17] Kim J Y, Lee B W, Read D T and Kwon D 2005 *Scr. Mater.* **52** 353
[18] Kim J Y, Kang S K, Lee J J, Jang J I, Lee Y H and Kwon D 2007 *Acta Mater.* **55** 3555